SYNTHESIS AND CHARACTERIZATIONOF TEMPERATURE SENSITIVEMAGNETIC FLUIDS

A thesis Submitted in the partial fulfilment of requirement for the award of the Degree of

Master of Science
In
Physics

Submitted by:

ShevaliGarg

(Regn. No.-300904016)

Under the guidance of

Dr. Bhupendrakumar Chudasama

School of Physics and Material sciences

THAPAR UNIVERSITY

PATIALA-147004

JULY 2011

Certificate

This is to certify that **Miss Shevali Garg** has worked on this thesis report entitled "**Synthesis and Characterization of Temperature Sensitive Magnetic Fluids**" in partial fulfilment of the requirements for the award of degree of **Masters of Science** in **Physics** in Thapar University, Patiala. This report is an authentic record of her own work carried out under the supervision of Dr. Bhupendrakumar Chudasama. The matter embodied in this report is one of the candidate's own record and not submitted to any other University in any part or full form for the award of such kind of degree.

B. Chudasama
07/07/2011

(Dr. Bhupendrakumar Chudasama)
Supervisor
School of Physics and Material Science
Thapar University
Patiala, INDIA

Countersigned by:

Dr. O. P. Pandey
Professor and Head
School of Physics and Materials Science
Thapar University
Patiala, INDIA

(Dr. S. K. Mohapatra)
Dean of academic affairs
Thapar University
Patiala, INDIA

ACKNOWLEDGEMENT

Knowledge in itself is a continuous process. I would have never succeeded in completing my task without the cooperation, encouragement and help provided to me by various personalities. With deep sense of gratitude, I express my sincere thanks to my esteemed and worthy supervisor Dr. Bhupendra Chudasama for his keen interest, strong motivation and constant encouragement during the course of the work. I thank him for his great patience and useful suggestion apart from invaluable guidance to me.

I am grateful to Dr. O.P. Pandey, Professor and Head for his encouragement and infrastructural facilities which he extended to me to execute this work.

I wish to express my sincere thanks to Dr. Kulvir Singh, Associate Professor, School of Physics and Materials Science, who have been a constant source of inspiration for me throughout this project work.

I would like to convey my sincere gratitude to my friends Ms Chandani, Mr. Paramjyot Jha, Mr. Jaspal Singh, Mr. Amit Bansal, Ms Samita and Mrs. Gurbinder Kaur Chaudhary for their support, timely help and valuable discussions. I extend my sincere thanks to all the staff members of School of Physics and Materials Science for their support and encouragement. I am also thankful to Dr. Rajesh Patel, Department of Physics, Bhavnagar University for VSM measurements.

Last but not the least, I am deeply thankful to my family, especially my mother Mrs. Raj Gupta, for all that they have done for me.

Above all, I render my gratitude to the Almighty God for his love and blessings.

Shevali Garg

(Shevali)

DEDICATED

TO

MY

LOVING PARENTS

ABSTRACT

The unusual magnetic properties exhibited by nanoparticles and their promising technological applications have attracted much interest in recent years. The magnetic fluid is considered to have applications in the field of heat transfer in solar systems and cooling of mechanical and electric heat sources. The Mn-Zn ferrite nanoparticles are used in the preparation of temperature sensitive magnetic fluid. The main aim of the present thesis is to prepare stable, sensitive magnetic fluid using Mn-Zn ferrite nanoparticles.

This report begins with a detailed description of magnetism, ferrites, ferrofluids and their important applications in chapter 1.Chapter 2 deals with relevant literature review to understand the state of art in the field. The detail methodology of synthesis of nanoparticles and magnetic fluids along with various characterization techniques are incorporated in chapter 3.In chapter 4, we have analysed the results obtained from various tests of nanoparticles. Formation of single-phase $Mn_{(1-x)}Zn_xFe_2O_4$ nanoparticles at low temperature was confirmed by XRD. It was confirmed from TGA analysis that monolayer coating of oleic acid was successfully achieved, which prevents agglomeration of nanoparticles. This fact is confirmed by TEM study. Magnetization measurement reveals that as the Zn content in the sample increases, the saturation magnetization of the sample decreases. Further, the samples prepared at higher pH are strongly magnetic than their counter parts prepared at lower pH. This can be understandable from the fact that the increasing pH results into better crystallinity and larger size.

The current study can be extended to prepare transformer oil based magnetic fluids, which has tremendous application potentials.

INDEX

CONTENTS **PAGE NO.**

LIST OF FIGURES

LIST OF TABLES

Chapter 1

INTRODUCTION

1.1 Magnetism

In atoms, the orbital motion of electrons around the nucleus and protons within the nucleus produce magnetic fields. In addition, the spinning motion of electrons, proton, and neutrons around their axes generate magnetic fields. However, because the contribution to the induced magnetic field of nucleons is typically two thousand times smaller than that of electrons, it is usually neglected. Many atoms have a permanent non-zero magnetic moment, of the order of 10^{-23} Am^2. The net magnetic moment of an assembly of atoms, however, is generally zero due the random orientation of atomic moments within the assembly (see figure 1.1a).

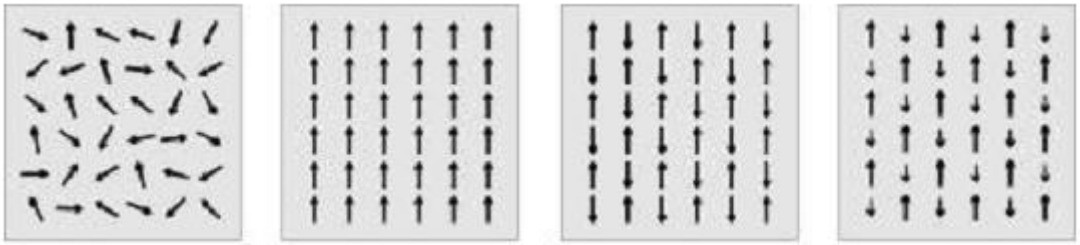

(a) (b) (c) (d)

Figure 1.1 Dipole orientations in four types of magnetic materials: (a) paramagnet (b) ferromagnet (c) antiferromagnet (d) ferrimagnet

The net magnetic moment can be changed by bringing the assembly into an external magnetic field H. This effect of Hcan usually be expressed as M = ᵡHwhere M is the magnetization (net dipole moment per unit volume) andᵡ the susceptibility, describing the strength of the response to an external magnetic field. Microscopically, the effect of the external field is twofold. First, the external field exerts a torque τ=mHon the atomic moments that forces them to align with H. Since, Brownian rotation counteracts the alignment; the degree of alignment depends on the magnetic field

strength and temperature. The alignment of dipoles with Hgives a positive contribution to χ, called the paramagneticsusceptibility. Second, the external field induceschange in the orbital motion of electrons, thereby producing a magnetic field that opposes the external field. Accordingly, this effect gives a negative contribution to χ,called the diamagneticsusceptibility. The diamagnetic susceptibility is independent of temperature and is present in all atoms, regardless of the presence of a permanent magnetic moment.Depending on the sign of the total susceptibility, materials are classified as paramagnets ($\chi>0$,$\chi\sim 10^{-5}$ to 10^{-3}) or diamantes ($\chi< 0$, $\chi\sim -10^{-5}$)[1-3].

1.1.1 Ferromagnetism, Antiferromagnetism and Ferrimagnetism

In the previous section, magnetic materials were treated as systems containing atoms with non interacting dipoles. In some materials, however, strong dipole-dipole interaction causes long range orientational correlations ofthe permanent atomic dipoles. In metallic iron, for example, dipolar interaction favours parallel alignment of the dipoles (figure 1.1b); hence this material has a net magnetization even in the absence of an external field. Materials with this kind of ordering of dipoles are called ferromagnets, and are characterized by high susceptibility, typically between 10^{-2} and 10^{6}, which, moreover, depends on the field strength. Above specific temperature, the dipolar ordering inside a ferromagnet is lost and the material becomes a paramagnet.

Dipolar interaction does not always lead to net magnetization. In some materials, named antiferromagnets, neighbouring dipoles are aligned antiparallel (figure 1.1c). Consequently, such materials do not have net magnetization in the absence of an external field and have low susceptibility,generally between 0 to 10^{-2}. At the so-called Neel temperature, a transition from antiferromagnet ordering to paramagnetic occurs [1, 2]**.**

Ferrimagnetsform a third class of magnetic materials with ordered dipoles. On the microscopic scale, ferrimagnets are similar to antiferromagnets, with antiparallel arrangement of neighbouring dipoles. However, because the number (or magnitude) of dipoles pointing in one direction differs from the number pointing in the opposite direction, ferrimagnets have a non-zero magnetization in zero field (figure 1.1d). Thus, ferrimagnets resemble ferromagnets on the macroscopic scale. Due to partial

cancellation of dipole moments, the magnetization of ferrimagnets is generally lower than that of ferromagnets. The most well-known ferrimagnetic material is magnetite (Fe_3O_4) [1, 2]**.**

1.1.2 Magnetic domains

The dipole ordering described in the previous section is long range, but usually does not extend over the entire volume of a sample. Rather, a sample of magnetic material is split up into domains in which all dipoles are ordered along a preferential direction (figure 1.2). This direction changes from domain to domain, and it is for this reason that bulk magnetic materials may be nonmagnetic, even though they are magnetic on the length scale of the domains.

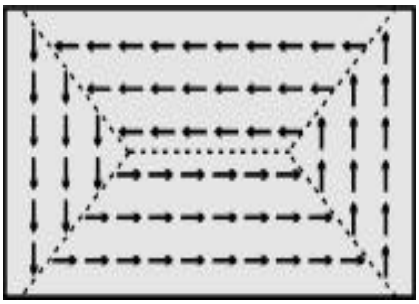

Figure1.2 In ferromagnetic materials, dipole alignment is split into domains

In an external magnetic field, the magnetization directions of the domains are forced to align with the external field, or domains with favourable magnetization direction will grow at the cost of domains with unfavourable directions. This increases the net magnetization of the bulk material. At infinite magnetic field strength, all dipoles are aligned with the field, and the system has reached its saturation magnetization. Once the field is removed, the magnetization tends to relax into its original state with random oriented domains. However, in order to reach that equilibrium state, the system may have to pass unfavourable states that can keep it from actually reaching equilibrium. Materials for which the relaxation to the unmagnified state is prevented are called hardmagnetic, as opposed to soft magneticmaterials, which demagnetize quickly upon removal of the external field or application of a small field opposing the magnetization [1, 3]**.**

1.2 Ferrites

Ferrites are the class of ferrimagnetic materials represented by the general formula $M^{2+}Fe^{3+}O_4$, where M is a divalent ion of a transition metal such as iron, cobalt, nickel, manganese, copper or zinc. A range of magnetic properties can be obtained through the choice of M, which may be a single metal species or a combination of two or more species. The variable properties include Curie temperature and saturation magnetization, defined as the maximum attainable magnetic moment per unit volume of material.

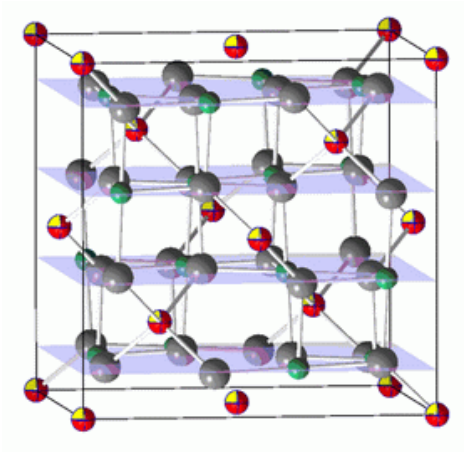

Figure 1.3 Structure of spinal ferrites

Ferrite particles can be used to prepare magnetic fluids. Most substituted ferrites tend to have Curie temperatures too high for practical use. However, many mixed ferrites exhibit Curie temperatures in the range of 100°-200° C. In addition, some orthoferrites and rare-earth garnets have acceptably low Curie temperatures.

Material	Curie Temperature (°C)
$Mn_{0.50}Zn_{0.50}Fe_2O_4$	150
$Ni_{0.3}Zn_{0.7}Fe_2O_4$	130
$Ni_{0.2}Zn_{0.6}Fe_{2.2}O_4$	145
$Zn_{0.6}Co_{0.5}Fe_{1.9}O_4$	115
$Mg_{0.5}Zn_{0.5}Fe_2O_4$	120
$MnFe_2O_4$	300

Table 1: Curie temperature of ferrite nanoparticles

1.2.1 Types of Ferrites

1) Soft Ferrites

Ferrites that have low coercivity are called soft ferrites. The low coercivity means the material's magnetization can easily reverse direction without dissipating much energy (hysteresis losses); while the material's high resistivity prevents eddy currents in the core, which is another source of energy loss. Major categories of soft ferrites are manganese-zinc and nickel-zinc ferrites.

2) Hard Ferrites:

Ferrites that have high coercivity and highremnantmagnetization are called hard ferrites. These are composed of iron and barium or strontium oxides. The high coercivity means the materials are resistant to demagnetized, an essential characteristic of a permanent magnet.

1.2.2 Mn-Zn ferrite

Manganese zinc ferrites are technologically important materials because of their high magnetic permeability and low core losses. These ferrite nanoparticles have been widely used in electronic applications such as transformers, choke coils, noise filters, recording heads, magnetic amplifiers and electromagnetic interference devices.[4] Recently, they are used to prepare temperature sensitive ferrofluids for applications in heat transfer enhancement and energy conversion devices.

Ferrites were previously produced by high temperature solid state reactions. The particles obtained by such a process are considerably large and non-uniform in size. Due to rapid development of nanotechnology and the unique features of Mn–Zn ferrite materials, several different methods have been proposed to prepare these nanoparticles. Among those, the co-precipitation method, the hydrothermal precipitation processing, the sol–gel synthesis, and the micro emulsions approach are often used to synthesize the Mn–Zn ferrite nanoparticles.

1.2.2 Introduction to spinel structure

The spinels are minerals of general formulation $A^{2+}B_2^{3+}O_4^{2-}$ which are cubic crystal structures, with the oxide anions arranged in a cubic close packing and the cations A and B occupying some or all of the octahedral and tetrahedral sites. A and B can be the same metal under different charges, such as the case in Fe_3O_4 (as $Fe^{2+}Fe_2^{3+}O_4^{2-}$).

Spinel group is classified as

Aluminium spinels

- Spinel – $MgAl_2O_4$, after which this class of minerals is named
- Gahnite - $ZnAl_2O_4$
- Hercynite - $FeAl_2O_4$

Iron spinels

- Cuprospinel - $CuFe_2O_4$
- Franklinite- $(Fe,Mn,Zn)(Fe,Mn)_2O_4$
- Jacobsite - $MnFe_2O_4$
- Magnetite - Fe_3O_4
- Trevorite - $NiFe_2O_4$
- Ulvospinel - $TiFe_2O_4$
- Zinc ferrite - (Zn, Fe) Fe_2O_4

There are many more compounds with a spinel structure.

Normal spinel structures are usually cubic closed-packed oxides with one octahedral and two tetrahedral sites per oxide. The tetrahedral points are smaller than the octahedral points. B^{3+} ions occupy the octahedral holes because of a charge factor, but can only occupy half of the octahedral holes. A^{2+} ions occupy 1/8 of the tetrahedral holes. This maximizes the lattice energy if the ions are similar in size. A common example of a normal spinel is $MgAl_2O_4$.

Inverse spinel structures are slightly different in that one must take into account the crystal field stabilization energies (CFSE) of the transition metals present. Some ions may have a distinct preference on the octahedral site which is dependent on the d-

electron count. If the A^{2+}ions have a strong preference for the octahedral site, they will force their way into it and displace half of the B^{3+} ions from the octahedral sites to the tetrahedral sites. If the B^{3+} ions have a low or zero octahedral site stabilization energy (OSSE), then they have no preference and will adopt the tetrahedral site. A common example of an inverse spinel is Fe_3O_4.

1.3Ferrofluids/Magnetic fluids

Ferrofluids are the colloidal suspension of ferro/ferri-magnetic particles of size range 2-10nm, coated with surfactant chains in a carrier liquid. The liquid can be polar or non-polar.It is stable against gravitational as well as magnetic field gradient. In the case of ferrofluid the solvent may be kerosene, hexadecane or water and oleic acid is generally used as a solvent.Oleic acid is a long chain hydrocarbon consist of polar head called hydrophobic part and a more extended hydrocarbon tail called hydrophilic part [5] .Oleic acid is one of the most widely used surfactants. The binding of oleic acid with magnetic particles is schematically presented in figure 1.3.

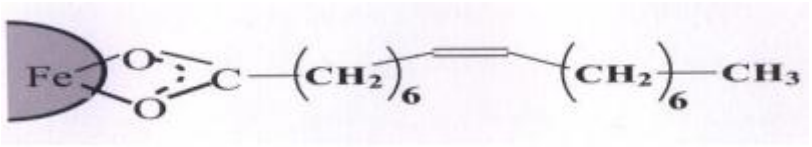

Figure 1.4 Binding of oleic acid with magnetic particles

Ferrofluids keep their fluidity even when subjected to strong magnetic fields.They become strongly magnetized in the present of a magnetic field. They don't retain magnetization in the absence of external magnetic field and thus are often classified as "superparamagnets" rather than ferromagnets. A prerequisite for a long-term stability is: particles should not aggregate, as aggregates sediment faster and have slower Brownian motion to compensate for sedimentation. Unfortunately, without special measures magnetic particles will form large clumps that settle quickly. To prevent aggregation, the colloids can be covered with a thin layer of polymer, commonly a monolayer of oleic acid, which makes the particles soluble in many organic solvents. Based on the type of coating, they are classified into two main groups

1)Surfacted ferrofluids

2) Ionic ferrofluids

1)**Surfaced Ferrofluids**

These magnetic fluids are stabilized by surfactants. Surfacted ferrofluids are formed by magnetic particles coated with surfactants (like oleic acid, louric acid, tetramethylammonium hydroxide, etc.) in order to prevent their agglomeration. Steric repulsion between particles acts as a physical barrier that keeps magnetic particles in the solution and stabilizes the colloid. If the particles are dispersed in a non-polar median, as oil, one layer of surfactant is sufficient to form hydrophobic layer. The polar head of the surfactant is attached tothe particle and chain is in contact with the fluid carrier. On the other hand, if the particles are dispersed in a polar median, a double layer of surfactant is required.

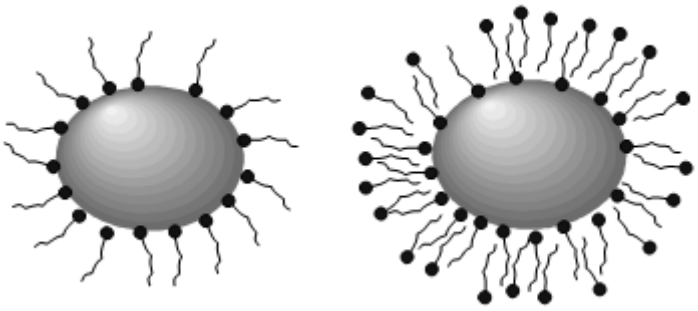

(a) (b)

Figure 1.5 Surfacted ferrofluid grain: (a) Single-layered grain (b) Double-layered

2) **Ionic ferrofluids**

In ionic ferrofluids, nanoparticles are electrically charged to keep the colloidal system stable. Magnetic particlesare obtained by co-precipitation method. Usually, the liquid carrier is water and the pH of the solution can vary from 2 to 12 depending on the sign of the surface charge of the particles. Acid ionic ferrofluid (pH<7) have positively chargedferrofluid particles, and alkaline ionic ferrofluid (pH>7) have negatively charged particles. The surface charged density of the particles is typically of the order of 10 $\mu c/cm^2$and it is a function of the solution pH [6].

1.4Applications of ferrofluids

1.4.1 Rotary shaft Seal

Rotary shaft seal is the most commercially exploited application of ferrofluids [7]. Between stationary housing and rotating shaft, 'O' ring(s) of ferrofluid is formed by a ring magnet and focussing pole structure. An 'O' ring can sustain certain pressure difference,which depends on saturation magnetization of the fluid,field gradient generated by the permanent ring magnet and pole structure[8].Such seals are used in rotating anode, X-ray generator,disc-drive system for computer, etc. [9]

1.4.2Medicine

In medicine, magnetic fluids are used as contrast agents for magnetic resonance imaging (MRI) and can be used for cancer detection.

There is also much experimentation with the use of magnetic fluids in an experimental cancer treatment called magnetic hyperthermia. It is based on the fact that a magnetic fluid placed in an alternating magnetic field releases heat.

1.4.2.1 Magnetic drug targeting

The major disadvantage of most chemotherapy is that they are relatively non-specific. The therapeutic drugs are administered intravenously leading to general systemic distribution, resulting in deleterious side-effects as the drug attacks normal, healthy cells in addition to the target tumour cells.For this purpose the use of magnetic carriers to target specific sites (generally cancerous tumours) within the body. The objectives are two-fold: (i) to reduce the amount of systemic distribution of the cytotoxic drug, thus reducing the associated side-effects; and (ii) to reduce the dosage required by more efficient, localized targeting of the drug.

In this therapy, a cytotoxic drug is attached to a biocompatible magnetic nanoparticle carrier. These drug/carrier complexes usually in the form of biocompatible magnetic fluidsare injected into the patient via the circulatory system. When the particles have entered the bloodstream, external, high-gradient magnetic fields are used to concentrate the complex at a specific target site within the body (Figure 1.7). Once the drug/carrier is concentrated at the target, the drug can be

released either via enzymatic activity or changes in physiological conditions such as pH, osmolality, or temperature, and be taken up by the tumour cells. [10]

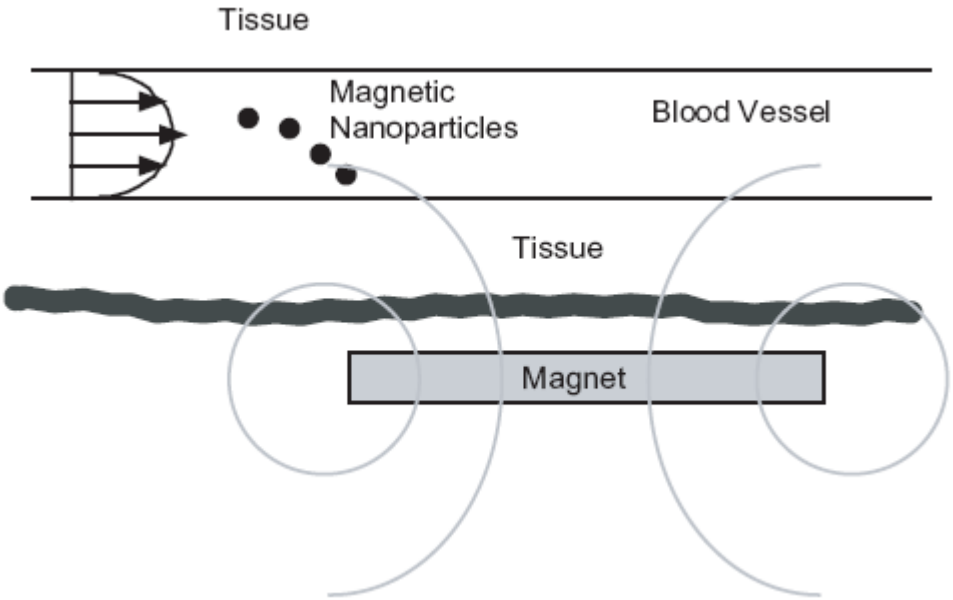

Figure 1.6A hypothetical magnetic drug delivery system shown in cross-section: a magnet is placed outside the body in order that its magnetic field gradient might capture magnetic carriers flowing in the circulatory system

1.4.2.2 Magnetic cell separation

In biomedicine it is often advantageous to separate out specific biological entities from their native environment magnetic separation using biocompatible nanoparticles is one way to achieve this. It is a two-step process, involving

(i) The tagging or labelling of the desired biological entity with magnetic material, and

(ii) The separating out of these tagged entities via a fluid-based magnetic separation device.

Tagging is made possible through chemical modification of the surface of the magnetic nanoparticles, usually by coating with biocompatible molecules such as dextran, polyvinyl alcohol (PVA) and phosopholipids. The magnetically labelled material is separated from its native solution by passing the fluid mixture through a

region in which there is a magnetic field gradient which can immobilize the tagged material via the magnetic force.

Magnetic separator design can be as simple as the application and removal of a permanent magnet to the wall of a test tube to cause aggregation, followed by removal of the supernatant (Figure 1.8(a)). A typical way to achieve this is to loosely pack a flow column with a magnetizable matrix of wire (e.g. steel wool) or beads and to pump the magnetically tagged fluid through the column while a field is applied (Figure 1.8(b)) [10].

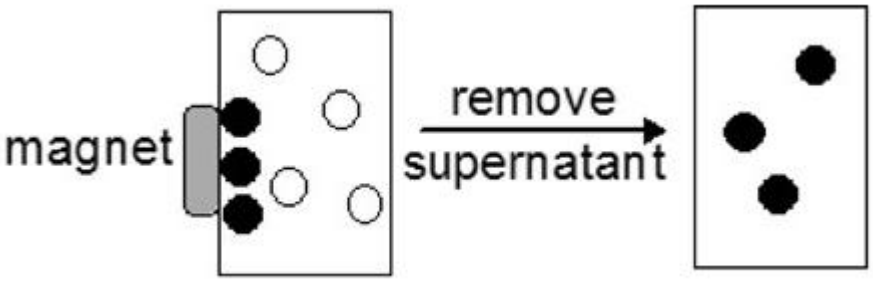

Figure 1.7(a) A magnet is attached to the container wall of a solution of magnetically tagged (•) and unwanted (◦) biomaterials. The tagged particles are gathered by the magnet, and the unwanted supernatant solution is removed

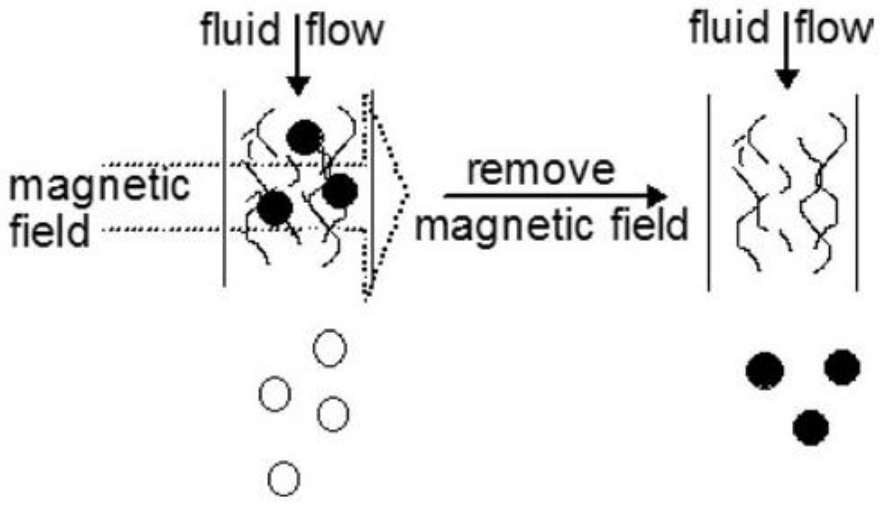

Figure 1.7(b) A solution containing tagged and unwanted biomaterials flows continuously through a region of strong magnetic field gradient, often provided by packing the column with steel wool, which captures the tagged particles. Thereafter the tagged articles are recovered by removing the field and flushing through with water [10].

1.4.3Material recycling

Ferrofluid has a unique property;applying magnetic field to the ferrofluid will increase its apparent density. This physical characteristic creates the ability to separate objects of different density through floatation or sinking. Ferrofluids have been used for years in material separation processes in the mining industries.

1.4.4Damper

Dampers are used in machinery to dissipate kinetic energy associated with vibrations and hence damp mechanical shocks and consequent vibrations. Conventional hydraulic dampers have constant damping, only in special cases their damping can be changed by regulation of fluid flow with a throttle valve. Ferro hydraulic dampers provide a more elegant solution. They are filled with ferrofluid that is exposed to the magnetic field of the coil induced by a controlled current. It changes the viscosity of the ferrofluids and the damping increases. The current signal is controlled by an on-line sensor that reads the causes of vibrations.

1.4.5Speakers with ferrofluid are constructed as common electrodynamic speakers: there is an air gap, in the magnetic circuit in which a coil vibrates that is fed by acoustic signal and connected with the membrane(figure 1.9). In ferrofluid based speakers, bythe influence of the strong magnetic field of permanent magnet the ferrofluid is permanently kept in the air gap. The acoustic performance is limited by the acceptable current load of the coil. As the thermal conductivity of ferrofluid is ten times higher than thermal conductivity of air, it increases the current density in the coil and thus the acoustic performance of the speaker [11].

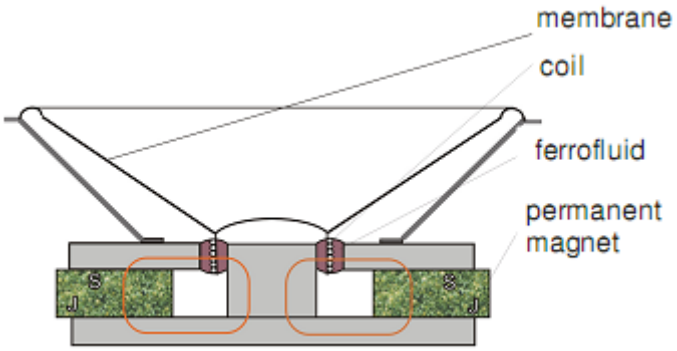

Figure 1.8 Speaker with ferrofluids in air gap

1.5 Temperature sensitive magnetic fluids:

Magnetic fluids whose magnetization strongly depends upon temperature are known as temperature sensitive magnetic fluids. Because of this thermo-magnetic property temperature sensitive magnetic fluids are considered as a promising fluid in energy conversion and heat transport system with small length scales or under micro gravity environment. [12]

Magnetically induced convention for thermal dissipation can be achieved by making use of temperature sensitive ferrofluids, magnetically responsive fluids having Mn-Zn ferrite nanoparticles are probable contender for heat transfer applications. Only close the Curie temperature, the adiabatic magnetization can cause considerable change in fluid temperature. In order to reduce the Curie temperature close to operating range $Mn_xZn_{(1-x)}Fe_2O_4$ particles are commonly used.

The temperature dependence of magnetization is very sensitive to the chemical composition of the ferrite. Thermomechanical analysis of the magnetic fluid suggests that the non-uniform magnetic field governs the thermoconvective processes and proper control of the same could make the fluid a very effective heat carrier [13].

1.5.1 Biomedical Application

The human body naturally uses heat to fight disease. Viruses and bacteria proliferate at normal body temperatures, so the body instinctively defends itself by increasing its temperature several degrees to slow the rapid multiplication of such disease-causing agents. This phenomenon, commonly called a fever, gives the body an advantage while fighting the infection. Fever form one subset of hyperthermia, an abnormally high body temperature. Hyperthermia also refers to body temperatures elevated for therapeutic reasons. The use of hyperthermia to treat many types of cancer has been a recent topic of research. Hyperthermia treatments elevate the temperatures of cancerous cells. Temperatures within the therapeutic temperature range, 42-45°C, improve the efficacy of other treatments like chemotherapy and radiotherapy. By raising the temperature to 45°C, hyperthermia alone can kill the cancerous cells. This latter treatment is usually referred to as thermal ablation. Hyperthermia can be performed by focusing laser, microwave, ultrasound or magnetic energy to the infected regions.

Gilchrist were the first to propose the use of magnetic materials in hyperthermia in 1957. He introduced magnetic microspheres into animal tissues and applied an alternating magnetic field. The alternating magnetic field can provide the energy necessary to reorient the particles' magnetic moments. Due to the phase lag between the magnetic moment and the applied magnetic field, magnetic energy is converted to thermal energy. Hyperthermia cancer treatment uses the heat generated by this conversion to destroy cancerous tissues. Temperatures above 42°C in healthy tissues can cause burns, blisters, and discomfort.

Consequentially, temperatures must be closely monitored during hyperthermia cancer treatment. The temperature that can be achieved in the tissue strongly depends on the properties of the magnetic material used, the frequency and the strength of the applied magnetic field, the blood perfusion in the tissue and the duration of application of the magnetic field. Therefore carefully chosen parameters and the means to monitor the real-time temperature are required. These complications can be eliminated by choosing a magnetic material that has a Curie temperature equal to the therapeutic temperature. At the Curie temperature ferromagnetic or ferrimagnetic materials (strongly magnetic) become paramagnetic (weakly magnetic). A magnetic material with a Curie temperature equal to the therapeutic temperature will act like a self-controller, generating heat only when below the therapeutic temperature. This therapy has been named self-regulated hyperthermia [14].

1.5.2 Engineering Application

1.5.2.1 Transformer cooling

Inductors represent a large class of electromagnetic devices. The simplest inductor, a solenoid, is merely a coil of wire, ordinarily wound around a core material. Current flowing through the wire creates a magnetic field within the core; when a voltage is applied across the inductor, the magnetic field causes the current to rise as a ramp, the slope of which depends on the strength, or inductance, of the device. Single-coil inductors are used, in many RF and tuned circuits. The core of an inductor is a hollow tube. However, winding the wire around a magnetic material augments the magnetic

field within the inductor, and therefore multiplies the inductance of the coil by the material's magnetic permeability.

Close coupling of two coils results into a transformer. Transformers are used to change an input voltage value to a different value for use in a particular application, and also serve to isolate electronic devices from their power sources. An AC voltage applied to first (or primary) coil appears across the other(or secondary) coil at an altered level determined by the ratio of wire turns in the primary and secondary coils. In transformers, the coils are frequently wound around different portions of the same core, resulting in maximum coupling between the windings.

Electricity supplied over long distances must ordinarily be provided at high voltage levels due to power losses in transmission. Large power transformers situated near delivery points are utilized to bring the voltage down to standard line levels. These transformers operate at very high power levels, typically in the megawatt range. The performance of such devices is necessarily limited by the temperature rise they experience, as well as by the magnetic saturation of the core. A typical high-voltage power transformer exhibits a maximum temperature tolerance of 110 °C and a maximum core saturation value of 20,000 Gauss.

Transformers generate heat through energy losses. A portion of input power is inevitably dissipated in the core, the windings, and the dielectric materials that insulate the windings, increasing the temperature of the transformer's environment. This, in turn, results in elevated resistance within the windings (which are generally copper), increased hysteresis losses within the core, decreased saturation magnetization of the core, and degradation of the transformer's insulation. Ultimately, these factors can lead to significant and permanent efficiency reductions.

To inhibit excessive temperature rise, high-voltage power transformers are usually cooled by surrounding them with mineral oil. The final, steady-state temperature of the transformer reflects equilibrium between power losses and the heat-dissipation properties of the oil. As the oil is heated it experiences a decrease in density; accordingly, oil in contact with the transformer coils absorbs the greatest amount of heat and, as a result, becomes least dense and rises relative to the surrounding oil. As the rising oil makes contact with the walls of the housing it

transfers heat thereto (and, ultimately, with the transformer's exterior environment), cooling and increasing in density. The cooled oil travels toward the bottom of the container, replacing heated oil rising from the windings. This natural convection, caused by the interplay of gravity and heat-induced density variations, represents the cooling mechanism most commonly utilized in commercial high-voltage power transformers.

Unfortunately, the gravitational forces that circulate the oil are relatively weak. Temperature gradients across oil reservoirs are often observed to be quite large, signifying relatively poor heat transfer. Transformer windings frequently develop “hot spots” (regions of intense heating due to ineffective cooling) that can cause insulation to quickly break down. To improve the efficiency of heat dissipation, transformers are frequently equipped with cooling fixtures (e.g., fins) on the outside of the transformer housing, and occasionally with pumping devices to circulate the oil within the housing. However, because oil pumps are cumbersome, consume power and require maintenance, they are not typically employed.

Magnetic fluids, as a cooling medium can significantly enhance the convection process. The magnetization of magnetic fluids is temperature-dependent, decreasing steadily until the fluid reaches a characteristic "Curie temperature" at which point it loses all magnetic strength.

Magnetic field ordinarily surrounds the windings and core of transformer. This "leakage" field occurs as a result of electrical currents in the windings, and reflects imperfect channelling of the magnetic flux into the core; its strength is greatest in the immediate vicinity of the windings and core, and falls off rapidly with increasing distance.

When the winding is immersed in a magnetic fluid, then the magnetic field gradient draws the magnetic fluids toward the device; however, because the device generates heat too, the temperature of the fluid rises as it approaches the device, resulting in loss of magnetic properties and decrease in density. The magnetic fluids rises as the gravitational effect of density reduction begins to overcome the weakening of magnetic attraction. Movement of hot magnetic fluids is assisted by the attraction exerted by the electromagnetic device on cooler, more intensely magnetic fluids,

which displaces the hot rising magnetic fluids as it travels toward the device. Movement away from the heat source and contact with the walls of the housing causes the hot magnetic fluids to cool and reacquire magnetization. This convection cycle, driven by magnetic and gravitational forces, involves much faster fluid flows and therefore greater cooling effects than are achieved with ordinary systems.

The per-degree decrease in magnetic strength of magnetic fluids is greatest as the temperature approaches the Curie point. Thus, choosing a magnetic fluids whose Curie temperature is close to the device's characteristic operating temperature (typically 70-300°C) results in the strongest convection, since the drop in the magnetic fluids' magnetization with increasing proximity to the device will be at or close to its maximum. By contrast, magnetic fluids with Curie temperatures well in excess of the device's operating temperature experience a much smaller decrease in magnetization as they approach the device, and therefore do not materially enhance the convection process; such materials are generally not suitable for transformer cooling. This approach could results in efficiency increases due to enhanced cooling (and consequent reduction in average operating temperature), as well as elimination of "hot spots" in the windings that might otherwise result in malfunction or shortened device life.

In general, magnetic materials suitable for use with high-power transformers have Curie temperatures that range from 70 °C to 300°C. Preferred average particle sizes range from 50 to 200 Å, with an average size of 100 Å, being particularly preferred in order to impart a high overall magnetic susceptibility [15].

Chapter 2

LITERATURE REVIEW

2.1 Methods of preparation

Ferrites with spinel structure form a group of technologically important materials. There are many methods for the preparation of ferrites. These methods are:

(1) Ball –milling

(2) Standard ceramic method

(3) Nitrate- citrate auto combustion method

(4) Micro-emulsion method

(5) In-situ method

(6) Hydrothermal precipitation

(7) Co-precipitation method

(1)Ball-milling

Z.G. Zheng et al. [16] in 2008 studied the synthesis, structure and magnetic properties of the nanocrystalline $Zn_xMn_{1-x}Fe_2O_4$ ($x = 0.1 - 0.9$) prepared by high-energy ball milling. Their structure and magnetic properties of Mn–Zn ferrites with various Zn content were investigated by means of X-ray diffraction (XRD), scanning electron microscopy and magnetic property measurement system. The XRD results indicate that the formed particles with associated strains are ultrafine in diameter of about 18 nm and the super paramagnetic particle sizes increase with the temperature. The lattice parameters increase proportionally with the increase of Mn content. The magnetic studies on the milled nanocrystalline $Zn_xMn_{1-x}Fe_2O_4$ samples show that the ultrafine zinc ferrites exhibit net magnetization with a super paramagnetic behavior at room temperature.

(2) Standard ceramic method

S. M. Attia et al. [17] in 2006 studied the cation distribution of Mn-Zn ferrite.A series of polycrystalline ferrite samples with the composition $Mn_xZn_{1-x}Fe_2O_4$ (x=0.0, 0.25, 0.5, 0.75, and 1.0) were prepared by the standard ceramic method. The crystal structures of all samples are cubic spinels. The lattice parameter a, increases with increasing Mn ion content; a = 8.419 Å for $ZnFe_2O_4$ and a = 8.478 Å for $MnFe_2O_4$. The average crystallite size was 31.5 nm.

Theoretical densityof ferrite decrease asMn content.The cation distribution was estimated by x–ray diffraction and Mossbauer spectra for all samples. The estimated cation distribution showed that Zn ion is mainly distributed over A site while Fe and Mn ions are distributed over A and B site. The Mossbauer spectra for the samples with x = 0.0 and 0.25 show central paramagnetic phase only. The spectra for the sample with x = 0.5 shows a central paramagnetic phase combined with weak six line Zeeman patterns. The spectra for the samples with x= 0.75 and 1.0 show six line Zeeman pattern only. The decrease of the hyperfine fields with increasing of Zn content was attributed to the decrease of the exchange interaction.

(3) Nitrate - citrate auto combustion method

Ping Hu et al. [18] in 2010 studied Heat treatment effects on microstructure and magnetic properties of Mn–Zn ferrite powders. Mn–Zn ferrite powders ($Mn_{0.5}Zn_{0.5}Fe_2O_4$) were prepared by the nitrate–citrate auto-combustion method and subsequently annealed in air or argon. The effects of heat treatment temperature on crystalline phase formation, microstructure and magnetic properties of Mn–Zn ferrite were investigated by X-ray diffraction, thermogravimetric and differential thermal analysis, scanning electron microscopy and vibrating sample magnetometer.

The crystallite size of auto–combusted ferrite powders is about 23.6 nm. Ferrites decomposed to Fe_2O_3 and Mn_2O_3 after annealing above 550 °C in air, and had poor magnetic properties. However, Fe_2O_3 and Mn_2O_3 were dissolved after ferrites annealing above 1100 °C. Moreover, the 1200 °C annealed sample showed pure ferrite phase, larger saturation magnetization (M_s = 48.15 emu g^{-1}) and lower coercivity (H_c= 51 Oe) compared with the auto-combusted ferrite powder (M_s = 44.32 emu g^{-1}, H_c= 70 Oe). The 600 °C air annealed sample had the largest saturation

magnetization (Ms = 56.37 emu g^{-1}) and the lowest coercivity (H_c= 32 Oe) due to the presence of pure ferrite spinel phase, its microstructure and crystallite size.

(4) Microemultion method

D Makovec et al. [19] in 2004 studied the preparation of Mn-Zn ferrite nanoparticles in water CTAB–hexanolmicro emulsions.The region of micro emulsion stability in the system was determined, using the titration method as a function of the temperature, type and concentration of solutes in the aqueous phase. The nanoparticles were prepared in a two-step process: the precipitation of the corresponding hydroxides, followed by oxidation of the Fe^{2+}.The particle size was controlled by the composition of the micro emulsion and the concentration of the reactants in the aqueous solution of the micro emulsion. The specific magnetization of the nanoparticles was found to depend mainly on particle size: ranging from 1.3 $emug^{-1}$ for particles of approximately 2 nm in size to 7.3 $emug^{-1}$ for particles of approximately 5 nm in size.

(5) In-situ method

M. Emad and M. Ewais et al. [20] in2008 studied in-situ synthesis of Mn-Zn ferrite ($Mn_{0.8}Zn_{0.2}Fe_2O_4$) by solid state reaction process. Stoichiometric amounts of high purity MnO_2, ZnO and Fe_2O_3 were applied. The influence of temperature and reaction time on the rate of ferrite formation was studied. The thermal analysis tests of mixed oxides indicated that the reaction started up at 900-1000 °C and completed at 1150 °C .The reaction products were characterized by measuring the bulk density, cold crushing strength and magnetic properties. It was observed that the reaction rate increased with temperature up to 1150 °C then decreased with further rise in temperature up to 1200 °C. The obtained results were rationalized based on the microstructure feature, porosity measurements and pore size analysis. Successful fabrication of dense Mn-Zn ferrite which has high crushing strength and magnetic properties at 1150 °C was processed**.**

(6) Hydrothermal precipitation

C. Rath et al. [21] in 1999 studied the synthesis of nanosize (9 – 12 nm) $Mn_{0.65}Zn_{0.35}Fe_2O_4$ particles from metal chloride solution through a hydrothermal precipitation route using aqueous ammonia, and their characterization by XRD, TEM and VSM are reported. While at lower pH, precipitation of Mn was incomplete, higher pH of precipitation led to Zn loss in the particles. The optimum pH for stoichiometric precipitation was found to lie around 10. The coercive force, $H_c$and the transition temperature, T_c were high as compared to reported bulk values and confirm the nanosize nature of the particles. The M versus T curve, instead of showing a monotonic drop of magnetization, showed a cusp before T_c. This cusp-like feature is shown to arise due to an irreversible phase transition involving cationic redistribution in the unit cell of the nanoparticles.

ChandanaRath et al. [22] in 2002 have reported the dependence on cation distribution of particle size, lattice parameter and magnetic properties in nanosizeMn-Zn ferrite for different degrees of Zn substitution prepared by hydrothermal precipitation method. In Mn_{1-x} $Zn_xFe_2O_4$ (x = 0 to 1) nanosize particles prepared through hydrothermal precipitation, they observe a decrease in a particle size from 13 to 4 nm with increasing Zn concentration from 0 to 1. At specific compositions within x = 0.35 and 0.5, the temperature dependence of the magnetization exhibits a cusp-like behaviour below the temperature at which the nanoparticles undergo a ferri to paramagnetic transition. The Curie temperature, of the nanoparticles is in the range of 175-500 °C, which is much higher than their corresponding bulk values. The microstructure and magnetic properties of Mn-Zn ferrites are shown to be influenced by two competing processes: (a) the strong chemical affinity of Zn^{+2} to the tetrahedral A site and (b) the metastable cation distribution in nanoparticles.

Jing Feng et al. [23] in 2007 studied the synthesis and characterization of $Mn_{(1-x)}$ $Zn_xFe_2O_4$ nanoparticles by hydrothermal synthesis at 200 °C for 12 h and characterized by X-ray diffraction (XRD), FESEM and vibrating sample magnetometer (VSM) techniques. The additions of Zn^{2+} ions content reduced the nanoparticles size. With the increase of Zn^{2+} ions content, the Curie temperatureincreased first and then decreased; when x = 0.3, the Tc reaches the maximum value (430 K). The results could be explained that the Zn^{2+} ions changed

spin ordering to increase the Tc in the range of $x \leq 0.3$, and magnetic properties were decreased because of increase of nonmagnetic Zn^{2+} ions in the range of $x > 0.3$.

(7) Co-precipitation method

Auzans et al. [24, 25] in 1999 have studied the preparation and properties of Mn-Zn ferrite nanoparticles used for ionic and surfacted ferrofluids with different degrees of Zn substitution prepared by co-precipitation method. By Increasing the degree of zinc substitution affects the contents of associated water in the particles and also leads to smaller size of synthesized particle. Magnetization of the ferrofluids significantly decreases when the degree of Zn substitution exceeds.

B. Jeyadevan et al. [26] in 2003 has studied the use of Mn-Zn ferrite for the preparation of temperature sensitive magnetic fluids by co-precipitation method. The magnetization of substituted ferrite nanoparticles depends mostly on parameters such as reaction temperature, pH of the suspension, initial molar concentration, etc. It should be noted that the curie temperature of the particles remained similar to the co-precipitated particles suggesting that the composition of the Mn-Zn ferrite particles has not been affected by the modified synthesis technique. The average particle diameter and magnetization of the particles increased from 9 to 12 nm and 37 to 50 emu/g, respectively. The higher magnetization resulted in a higher magnetization temperature gradient and could serve as a potential candidate for preparation of temperature sensitive magnetic fluids.

R. Arulmurugan et al. [27] in 2005 studied effect of zinc substitution on Co-Zn and Mn-Zn ferrite nanoparticles prepared by co-precipitation. $Mn_{(1-x)}Zn_xFe_2O_4$ (x = 0.1 - 0.5) nanoparticles less than 12 nm are prepared by chemical Co-precipitation method which could be used for ferrofluid preparation. The saturation magnetization of the Co–Zn substituted ferrite nanoparticles decreases continuously with the increase in Zn concentration, whereas for the Mn-Zn substituted ferrite nanoparticles the saturation magnetization was maximum for x = 0.2 and decrease on further increase in Zn concentration. The particle size decreases with the increase in the Zn concentration for Mn-Zn ferrite. The estimation of associated water content, which increases with the Zn concentration, plays a vital role for the correct determination of cation contents. The Curie temperature and the temperature at which maximum value of thermomagnetic coefficient is observed decrease with the increase in Zn

concentration. Thermomagnetic coefficient calculated for $Mn_{(1-x)}Zn_xFe_2O_4$ has maximum value of 0.2 when x = 0.3 - 0.5.

B. ParvatheeswaraRao et al. [28] in 2006 studied the structural and magnetic characterizations of co-precipitated Mn-Zn ferrite nanoparticles. $Mn_{0.75}Zn_{0.18}Fe_2O_4$ have been prepared by co-precipitation method, and then the resulting ultrafine powders were heat treated at different temperature from 200 to 800°C for improved crystallinity and magnetic properties. As a result of heat treatment, the average particle size has been found to increase from 2.4 to 10.2 nm for Mn-Zn Ferrite, and the corresponding magnetization values have increased from 7.9 to 11.7 emu/g for Mn-Zn ferrite, respectively.

P. Mathur et al. [29] in 2007 studied the low temperature processing of Mn-Zn nanoferrites prepared by co-precipitation method. D.C resistivity is studied as a function of temperature and values up to 10^2 times greater than those for samples prepared by the conventional ceramic method are observed .It is found that resistivity decreases with increase in temperature .The initial permeability values are high as compared to those prepared by soft chemical route. Appreciable value of initial permeability was obtained at low temperature and permeability loss factors were also found remarkably low. The particle size is calculated using Scherrer equation for Lorentzian peak, which comes out between 9 nm and 19 nm.

Lai Zhenyu et al. [30] in 2007 studied microwave assisted low temperature synthesis of Mn-Zn ferrite nanoparticles. the reveals that $MnZnFe_2O_4$ ferrite nanoparticles were prepared by co-precipitation method using a microwave heating system at temperature of 100°C .X-ray diffraction reveals the samples as prepared are pure ferrite nanocrystalline phase, transmission electron microscopy image analysis shows particles are in agglomeration state and having spherical shape with an average size of about 10 nm, furthermore, crystal size of samples are increased with longer microwave heating.

Chapter 3

EXPERIMENTAL TECHNIQUES

3.1 Synthesis of $Mn_XZn_{1-X}Fe_2O_4$ nanoparticles

Various preparation techniques have been used for the synthesis of fine particles of ferrite, which exhibit novel properties when compared with bulk. Chemical methods such as co-precipitation, thermal decomposition, sol-gel and hydrothermal methods have been widely used to prepare ferrite nanoparticles. In the present work, conventional preparation method, known as co-precipitation was used for preparation of $Mn_XZn_{1-X}Fe_2O_4$. Main advantages of this method are:

It is inexpensive

Time saving

Processed at much lower temperature

3.1.1 Material

For this synthesis, manganeous chloride tetrahydrate, zinc sulphate heptahydrate, ferricchloridehexahydrate and sodium hydroxide were used, which was obtained from Merck, High purity extrapure kerosene (EPK) was obtained locally. Double distilled water is used to prepare all the solutions. All the chemicals were used as received without any purification.

3.1.2 Preparation of $Mn_{(1-x)}Zn_xFe_2O_4$ nanoparticles

Nanoparticles of $Mn_{(1-x)}Zn_xFe_2O_4$ with x = 0, x = 0.2, x = 0.4 and x = 0.5 were prepared by co-precipitation method. Requisite quantity of aqueous solution of 0.05M $Mncl_2.4H_2O$ was mixed with 0.05M aqueous solution of $ZnSO_4.7H_2O$. Colour of the mixture was transparent. Now 0.1M $FeCl_3.6H_2O$ dissolved in 200 ml distilled water was added to the previous mixture under constant magnetic stirring. Upon the addition of $FeCl_3.6H_2O$, the colour of the mixture immediately turned to

light yellow. The pH of this mixture should be less than 2 we use NaOH as co-precipitating agent. Mixed solution of $Mncl_2.4H_2O$, $ZnSO_4.7H_2O$ and $FeCl_3.6H_2O$ was added to the solution of NaOH (0.4M dissolved in 400 ml of distilled water) within 10 s under constant mechanical stirring. The colour of this mixture turned dark brown. The pH of this mixture was adjusted to 13 with excess NaOH solution. Stirr the mixture for 20 minutes. Following reaction were take place

$$0.5\ Mncl_2.4H_2O + 0.5\ ZnSO_4.7H_2O + 2\ FeCl_3.6H_2O + 8\ NaOH \rightarrow Mn_{0.5}Zn_{0.5}Fe_2O_4 + 7\ Nacl + 0.5\ Na_2SO_4 + 21.5\ H_2O$$

Nanoparticles were formed by conversion of metal salts into hydroxides, which take place immediately. The solution was maintained at 90 °c for 1 hour with constant stirring. This duration was sufficient for the transformation of hydroxides into spinal ferrite. The reaction vessel was cooled to room temperature and magnetically decanted. After that several water washes each of 200 ml were given followed by acetone washes of 100 ml each. During synthesis, molar concentration, temperature and PH of the reaction mixture were optimized to get a single-phase nano -crystalline materials [31].

3.1.3 Preparation of magnetic fluid:

Nanoparticles of $Mn_{(1-x)}Zn_xFe_2O_4$ with x varying from 0 to 0.5 were prepared by co-precipitation method. Hydrocarbon based ferrofluids were prepared from the precipitated fine particles directly by using oleic acid as the surfactant. Oleic acid was converted to sodium oleate and was transferred to the reaction vessel.

-

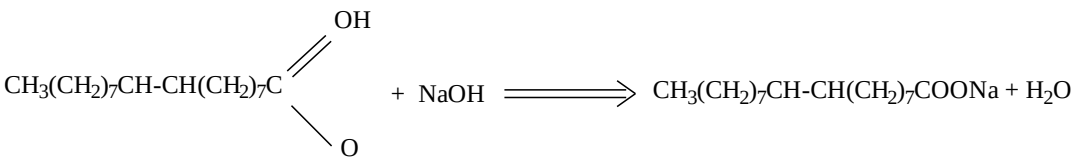

Stirring was continue for 1 h and coating of surfactant was carried out at 93°C. To coagulate the oleic acid-coated particles, dilute Hcl was added until the pH of the solution falls below 5. After decantation, the resulting product was washed many times with distilled water to remove water soluble impurities and unreacted

compounds. Finally water was removed by washing nanoparticles with acetone. This acetone –wet slurry was dispersed in 20 ml of High purity extrapure kerosene (EPK) and stirred for 1 hr under mild heating (50°C). The resulting fluid was centrifuged at 5000 rpm for 10 min to remove clusters of magnetic particles, if any [32].

3.2 Characterization techniques:

The composition, morphology, magnetic properties, and sizes of the synthesized nanoparticles were analysed by X-Ray diffraction, Transmission Electron Microscope, Vibrating sample magnetometer and Thermogravimetric analysis.

3.2.1 X-ray diffraction (XRD)

X-ray Diffraction (XRD) is a powerful non-destructive technique for characterizing crystalline materials. It provides information on structures, phases, preferred crystal orientations, and other structural parameters, such as average grain size, crystallinity, strain, and crystal defects. X-ray diffraction peaks are produced by constructive interference of monochromatic beam of x-rays scattered at specific angles from each set of lattice planes in a sample. The phenomenon is called X-ray diffraction.

3.2.1.1Working

X ray diffractometers consist of three basic elements: an X-ray tube, a sample holder, and an X-ray detector. X-rays are generated in a cathode ray tube by heating a filament to produce electrons, accelerating the electrons toward a target by applying a voltage, and bombarding the target material with electrons. When electrons have sufficient energy to dislodge inner shell electrons of the target material, characteristic X-rays are produced. These spectra consist of several components, the most common being K_α and K_β. K_α consists, in part, of $K_{\alpha1}$ and $K_{\alpha2}$. $K_{\alpha1}$ has a slightly shorter wavelength and twice the intensity as $K_{\alpha2}$. The specific wavelengths are characteristic of the target material (Cu, Fe, Mo, and Cr).

Filtering, by foils or crystal monochrometers, is required to produce monochromatic X-rays needed for diffraction. $K_{\alpha1}$and $K_{\alpha2}$ is sufficiently close in wavelength such that a weighted average of the two is used. Copper is the most common target material for

single-crystal diffraction, with Cu K_α radiation = 1.5418 Å. These X-rays are collimated and directed onto the sample. As the sample and detector are rotated, the intensity of the reflected X-rays is recorded. When the geometry of the incident X-rays impinging the sample satisfies the Bragg equation, constructive interference occurs and a peak in intensity is observed. A detector records and processes this X-ray signal and converts it to a count rate which is then output to a device such as a printer or computer monitor. The geometry of an X-ray diffractometer is such that the sample rotates in the path of the collimated X-ray beam at an angle θ while the X-ray detector is mounted on an arm to collect the diffracted X-rays and rotates at an angle of 2θ. The instrument used to maintain the angle and rotate the sample is termed a *goniometer.*

Figure3.1 The PANanaltical XRD X'pertPRO

When an X-ray beam hits a sample and is diffracted, we can measure the distances between the planes of the atoms that constitute the sample by applying Bragg's Law.

$$n\lambda = 2d\sin\theta,$$

where n is an integer, λ is the wavelength of incident wave, d is the lattice spacing and θ is the angle between the incident ray and the scattering planes. The

characteristic set of d-spacings generated in a typical X-ray scan provides a unique "fingerprint" of the mineral present in the sample. When
properly interpreted, by comparison with standard reference patterns, this "fingerprint" allows for identification of the material [33].

3.2.1.2 Applications

• To identify crystalline phases and orientation

• To determine crystal structure

• To determine lattice parameters, strain, grain size, expitaxy, phase composition, preferred orientation order disorder transformation, thermal expansion etc

• To measure thickness of thin films and multi-layers

3.2.2 Thermal Gravimetric Analysis (TGA)

Thermogravimetric analysis (TGA) is the most widely used thermal analysis method. It is based on the measurement of mass loss of material as a function of temperature. In thermogravimetry a continuous graph of mass change against temperature is obtained when a substance is heated at a uniform rate or kept at constant temperature. A plot of mass change versus temperature (T) is referred to as the thermogravimetric curve (TG curve).

Figure 3.2 Perkin Elmer TGA analyzer

3.2.2.1 Principle of Operation

Small amount of a sample is placed in a quartz boat, which is suspended from one arm of a sensitive electrobalance. The suspended sample boat hangs inside a glass walled, computer controlled furnace, with gas tight fittings. A thermocouple, which is used to monitor the temperature at the sample, is also located in the furnace next to the sample boat. The furnace, electrobalance, thermocouple and gas flow controllers are monitored and commanded by PC software, allowing independent programming of constant temperature and temperature ramp segments, along with switching different gases during a run. Under the selected conditions, different organic and inorganic components are evolved or decomposed, leading to a mass loss which is measured by the electrobalance [34].

3.2.2.2 Applications of thermogravimetric analysis

Purity and thermal stability
Solid state reactions
Decomposition of inorganic and organic compounds
Determining composition of the mixture
Corrosion of metals in various atmospheres
Roasting and calcinations of minerals
Reaction kinetics studies
Oxidative and reductive stability
Determining moisture, volatile and ash contents

3.2.3Vibrating sample magnetometer (VSM)

The vibrating sample magnetometer has become a widely used instrument for determining magnetic properties of a large variety of materials: diamagnetic, paramagnetic, ferromagnetic and antiferromagnetic. This experimental technique was invented in 1956 by Simon Foner, a scientist of the MIT.

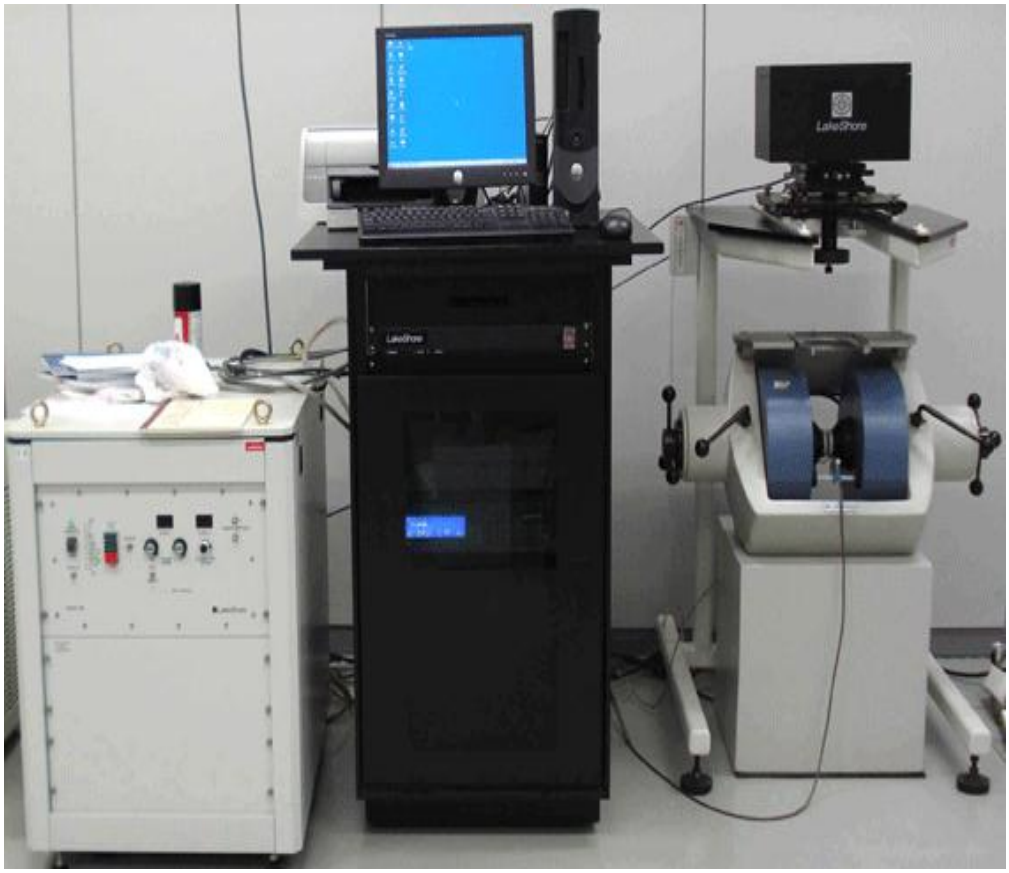

Figure 3.3 VSM Tamakawa model TM-VSM 1230-HHHS

3.2.3.1 Principle

A vibrating sample magnetometer (VSM) operates on Faraday's Law of Induction, which tells that a changing magnetic field will produce an electric field. This electric field can be measured and can tell us information about the changing magnetic field.

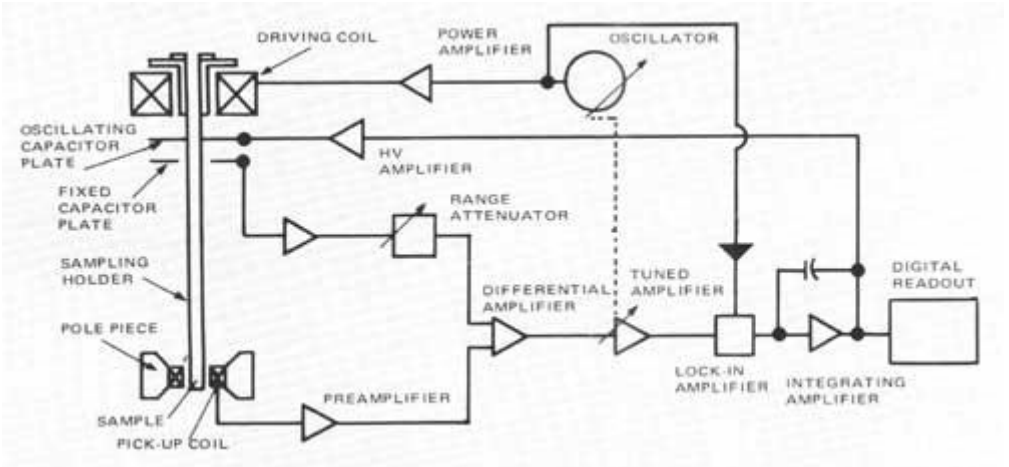

Figure3.4 Vibrating sample magnetometer block diagram.

3.2.3.2 Operation

If a sample is placed in a uniform magnetic field, created between the poles of electromagnet, a dipole moment will be induced proportional to the product of the sample susceptibility and the applied field. If the sample vibrates with sinusoidal motion a sinusoidal electrical signal can be induced in pick-up coils. The signal has the same frequency of vibration and its amplitude will be proportional to the magnetic moment.

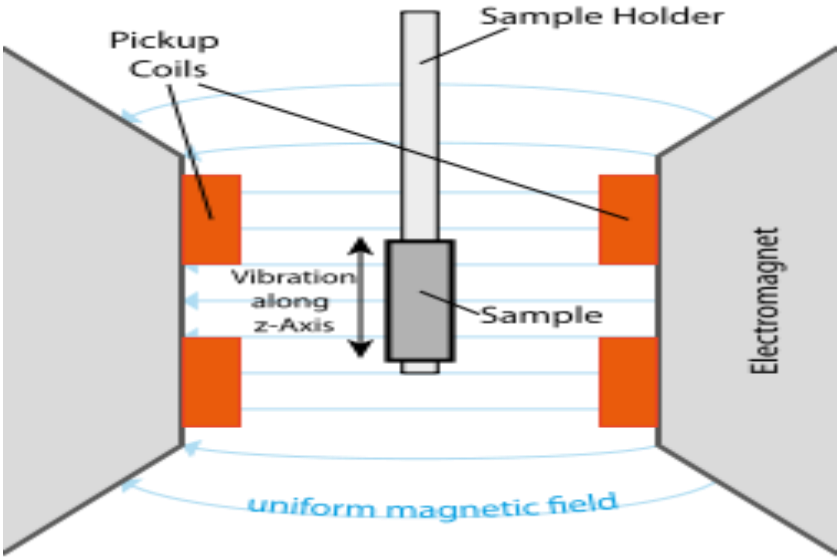

Figure3.5 Illustration of principle of VSM

The material under study in the VSM is inserted in the sample holder so that it rests cantered in a pair of pickup coils between the poles of an electromagnet. The sample holder is mounted using a sample rod in a transducer assembly which passes through the centre of a driving coil. The transducer is driven by a power amplifier which itself is driven by an oscillator at a frequency of 71 Hertz. The magnetic sample vibrates along the z-axis perpendicular to the magnetizing field. As it does so, it induces a signal in the sample pickup coils as described above. The magnitude of this signal is dependent on the magnetic properties of the sample itself.

Pair of stationary coils picks up the induced ac signal, which is proportional to the amplitude and frequency of the vibration and is used as a control signal for

modulation of the transducer. The output of the sample coil is fed to the differential input of a lock-in amplifier. The reference input of the lock-in comes from the sine wave oscillator used to drive the sample holder. The output of the lock-in goes to the data acquisition computer as well as the magnitude of the applied magnetic field coming from a gauss meter. The signal from the lock-in amplifier is directly proportional to the magnetic moment of the sample. The computer is now able to graph the magnetic moment of the sample against the applied magnetic field. [35]

3.2.4Transmission Electron Microscope (TEM):

Transmission Electron Microscopy (TEM) has become a major support tool in the list of characterization techniques for materials scientists. TEM's has high lateral spatial resolution (better than 0.2 nm "point-to-point'') and it has capability to produce both image and diffraction information from a single sample. In addition, the highly energetic beam of electrons used in TEM interacts with sample matter to produce characteristic radiation. These signals are analysed to determine materials characterization.

3.2.4.1 Principle of operation

The transmission electron microscope (TEM) forms an image by accelerating a beam of electrons that pass through the specimen. In TEM, electrons are accelerated to 100 KeV or higher (up to 1MeV), projected onto a thin specimen (less than 200 nm) by means of the condenser lens system, and penetrate the sample thickness either undeflected or deflected. The greatest advantages that TEM offers are the high magnification ranging from 50 to 10^6 and its ability to provide both image and diffraction information from a single sample.

The scattering processes experienced by electrons during their passage through the specimen determine the kind of information obtained. Elastic scattering involves no energy loss and gives rise to diffraction patterns. Inelastic interactions between primary electrons and sample electrons at heterogeneities such as grain boundaries, dislocations, second phase particles, defects, density variations, etc., cause complex absorption and scattering effects, leading to a spatial variation in the intensity of the transmitted electrons. In TEM one can switch between imaging the

sample and viewing its diffraction pattern by changing the strength of the intermediate lens.

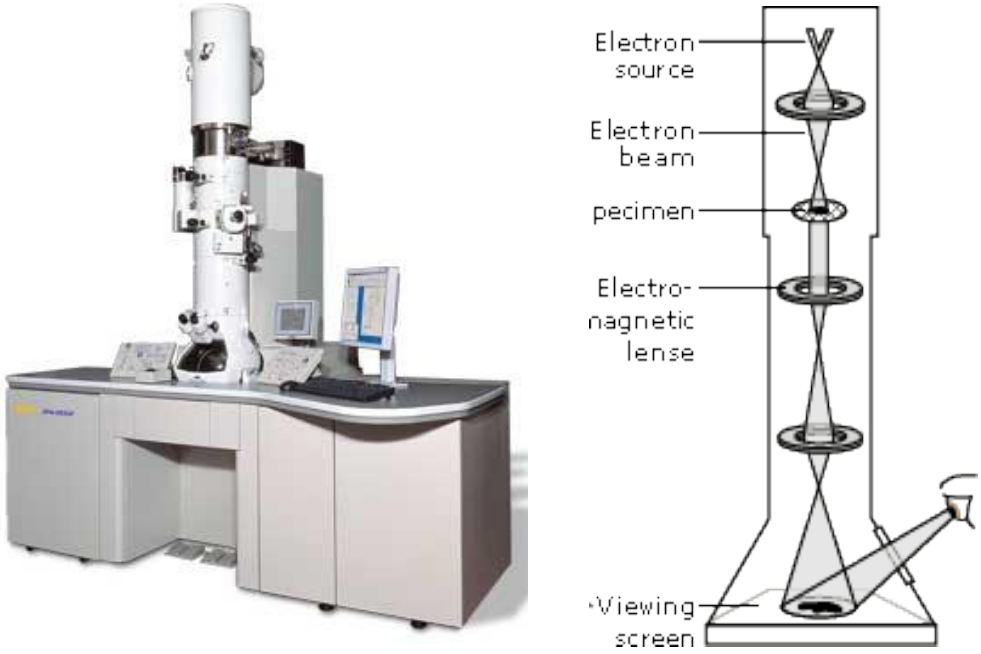

(a) (b)

Figure3.6 (a) GEOL GEM 200 HRTEM(b) Schematic ray diagram of TEM

One short coming of TEM is its limited depth resolution. Electron scattering information in a TEM image originates from a three-dimensional sample, but is projected onto a two dimensional detector. Therefore, structure information along the electron beam direction is superimposed at the image plane. Although the most difficult aspect of the TEM technique is the preparation of samples.

In addition to the capability of structural characterization and chemical analyses, TEM also has been explored for other applications in nanotechnology. Examples include the determination of melting points of nanocrystals, in which, an electron beam is used to heat up the nanocrystals and the melting points are determined by the disappearance of electron diffraction. Another example is the measurement of mechanical and electrical properties of individual nanowires and nanotubes. This technique allows a one-to-one correlation between the structure and properties of the nanowires [36].

Chapter 4

RESULTS AND DISCUSSIONS

Characterization of $Mn_XZn_{(1-X)}Fe_2O_4$ nanoparticles

In this chapter, we discuss results obtained from X-ray diffraction, Transmission electron Microscopy (TEM), Thermogravity and Magnetization measurements on Vibrating sample Magnetometer (VSM) of $Mn_XZn_{(1-X)}Fe_2O_4$nanoparticles.

4.1 Structural and Morphological Analysis

4.1.1 XRD Analysis

In figure 4.1, XRD Pattern of $MnFe_2O_4$ nanoparticles were presented as function of pH from 10.5 to 13.5. Clearly, from this figure, we observe that $MnFe_2O_4$ nanoparticles shows crystalline phase at pH values 12.5,13.0 and 13.5 and shows amorphous nature below 12.5.The peaks positioned at 29.8°, 35°, 42.6°, 56.2°, 61.8° were index to (220), (311), (400), (511), (440) crystal planes, respectively. The observed diffraction peaks were correspond to those of standard pattern of Manganese ferrite [37] with no extra lines indicating that the samples have single-phase inverse spinel structure and no other phase was present in these samples. As shown in the table 2, average crystallite size obtained by classical Scherrer equation with a geometrical factor of 0.9 over (311) at pH (12.5, 13.0 and 13.5) lies between 17.5 nm to 20 nm.

In figure 4.2, XRD pattern of $Mn_{0.8}Zn_{0.2}Fe_2O_4$ nanoparticles were presented as function of pH. In this figure, only (311) peak was observed. This might be due to poor crystallinity of the samples. The average crystallite size was calculated from the peak broadning of the (311) peak at pH 13.5 which comes out to be 15 nm.

From table 2, it can be concluded that the particle size decreases as the Znconcentration increases. The average particle size of $MnFe_2O_4$ nanoparticles is 20 nm at pH = 13.5 which decreases with the increasing Zn concentration and becomes 15.7 nm in case of $Mn_{0.8}Zn_{0.2}Fe_2O_4$ nanoparticles.

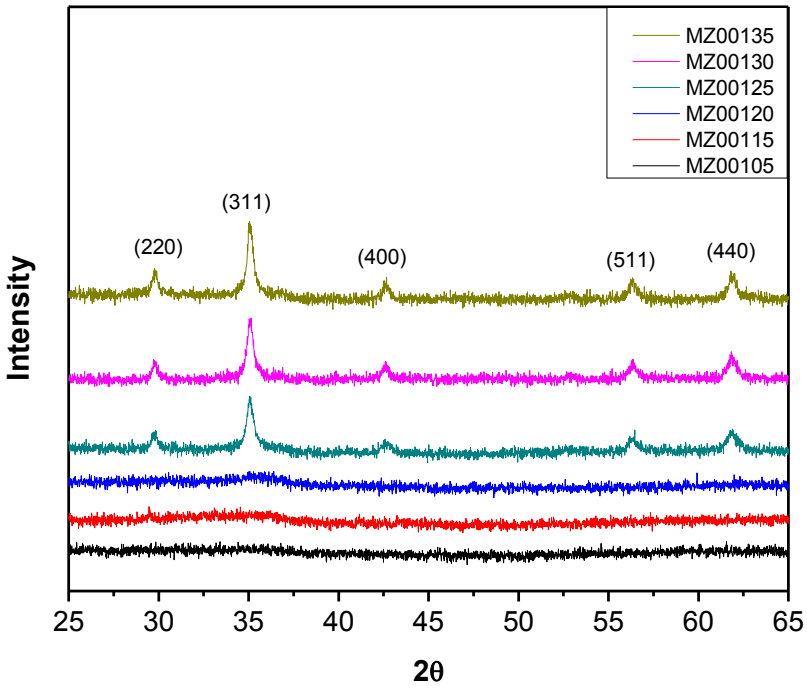

Figure 4.1 XRD patterns of $MnFe_2O_4$ nanoparticles

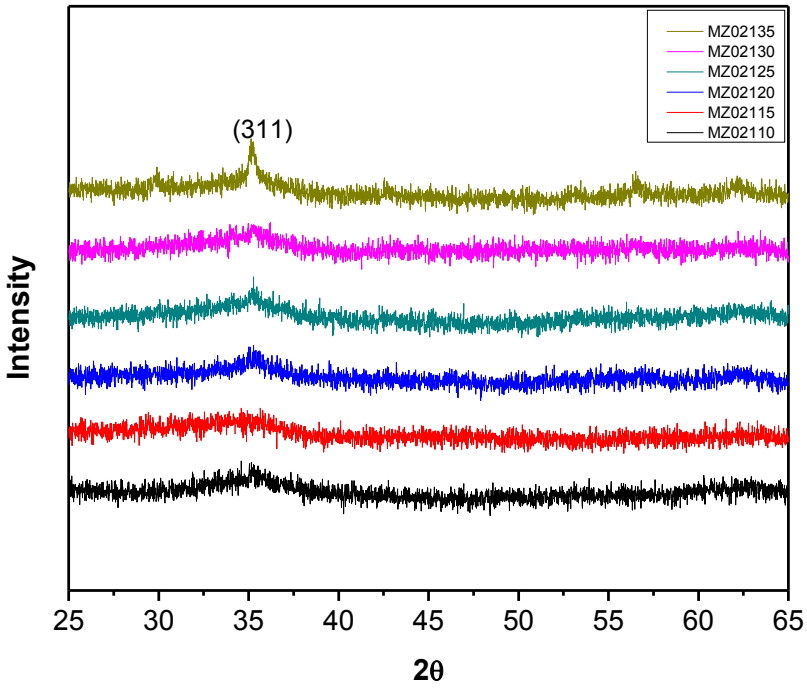

Figure 4.2 XRD patterns of $Mn_{0.8}Zn_{0.2}Fe_2O_4$ nanoparticle

From figure 4.3 and 4.4, we observe that as we further increase the Zinc concentration, the crystalline phase of structure disappears and only amorphous nature is observed.

S.NO	SAMPLE CODE	pH VALUE	X-RAY SIZE
1	MZ00105	10.5	--
2	MZ00115	11.5	--
3	MZ00120	12.0	--
4	MZ00125	12.5	17.5 nm
5	MZ00130	13.0	18.6 nm
6	MZ00135	13.5	20 nm
7	MZ02110	11.0	--
8	MZ02115	11.5	--
9	MZ02120	12.0	--
10	MZ02125	12.5	--
11	MZ02130	13.0	--
12	MZ02135	13.5	15.7 nm
13	MZ04115	11.5	--
14	MZ04120	12.0	--
15	MZ04125	12.5	--
16	MZ04135	13.5	--
17	MZ05130	13.0	--
18	MZ05135	13.5	--

Table 2 Effect of Zn concentration and pH on size of $Mn_{(1-x)}Zn_xFe_2O_4$ nanoparticles

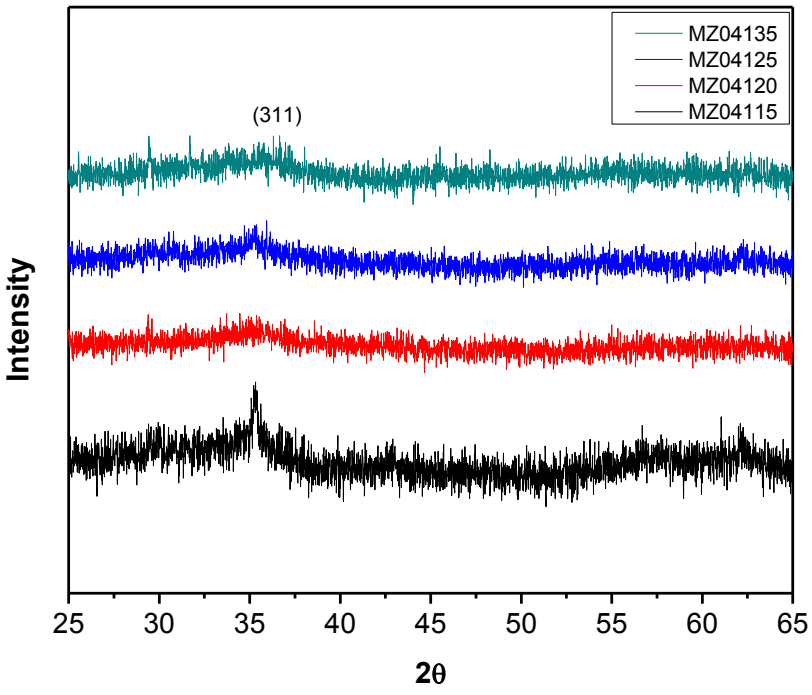

Figure 4.3 XRD patterns of $Mn_{0.6}Zn_{0.4}Fe_2O_4$ nanoparticles

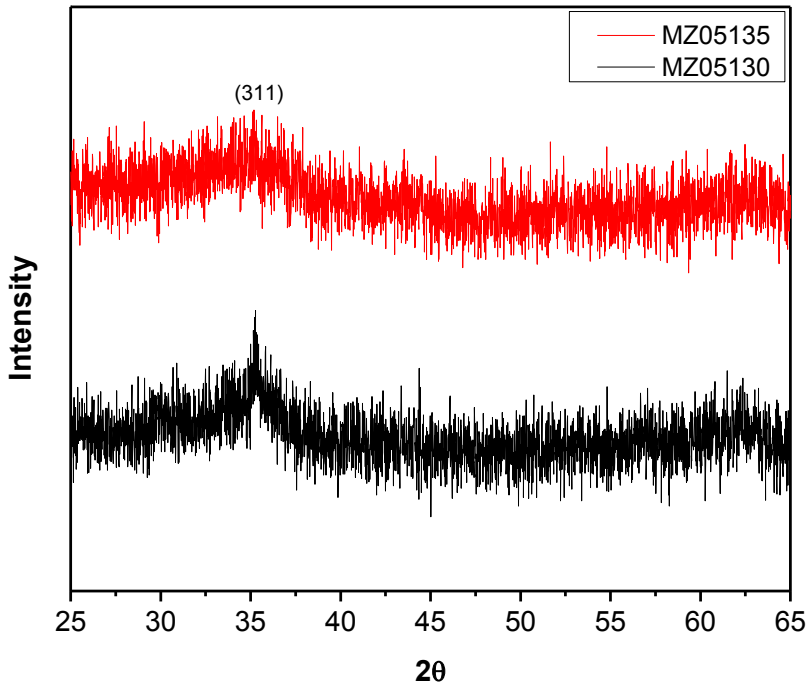

Figure 4.4 XRD patterns of $Mn_{0.5}Zn_{0.5}Fe_2O_4$nanoparticles

4.1.2 TEM Analysis

Tem Analysis of $Mn_{0.5}Zn_{0.5}Fe_2O_4$ nanoparticles is carried out on GEOL make GEM 200 high resolution electron microscope. From figure 4.6, we can see that particles are nearly spherical and average size is ~11.37 nm and polydispersity index is 2 %. It is clear from the figure that there is no agglomeration in the sample as individual particles are observed.

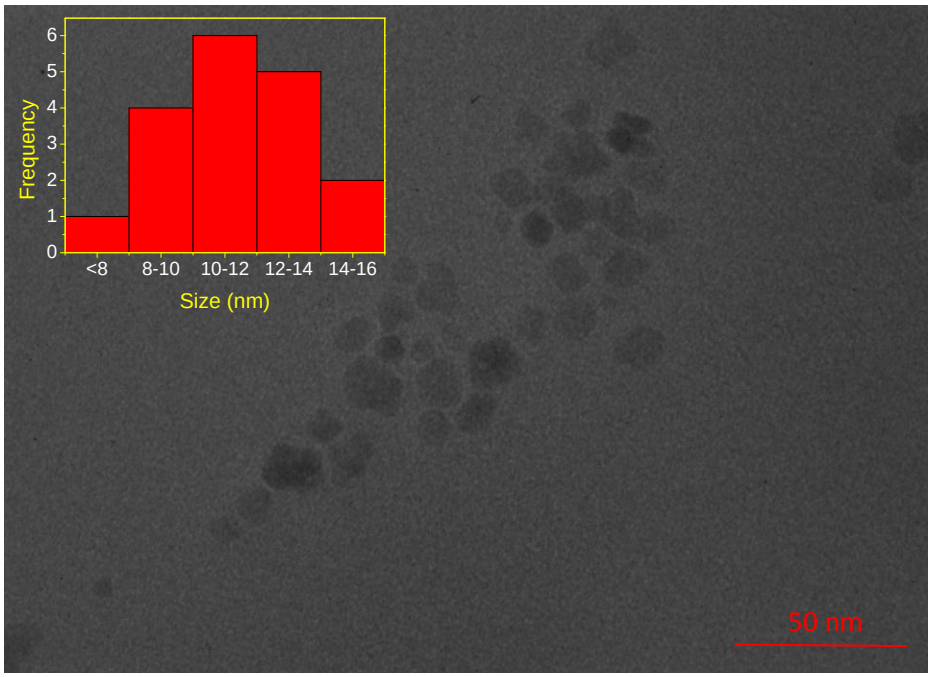

Figure 4.5 TEM image of $Mn_{0.5}Zn_{0.5}Fe_2O_4$ nanoparticles

4.2 Thermal analysis

TGA/DTA curves of oleic acid coated $MnFe_2O_4$ nanoparticles are shown in figure 4.5. From room temp to 100 °C, 2.31% weight loss is observed, which corresponds to removal of surface water. A sharp single step weigh loss of 30.4% was observed in the temperature range of 100 °C – 400 °C, which corresponds to decomposition of oleic acid. This weight loss corresponds to monolayer coating of oleic acid [38].In the DTA curve, a single peak is observed which is cantered at 246.48 °C. This indicates that the decomposition of oleic acid is a single step process. The rate of decomposition is highest at 246 °C.

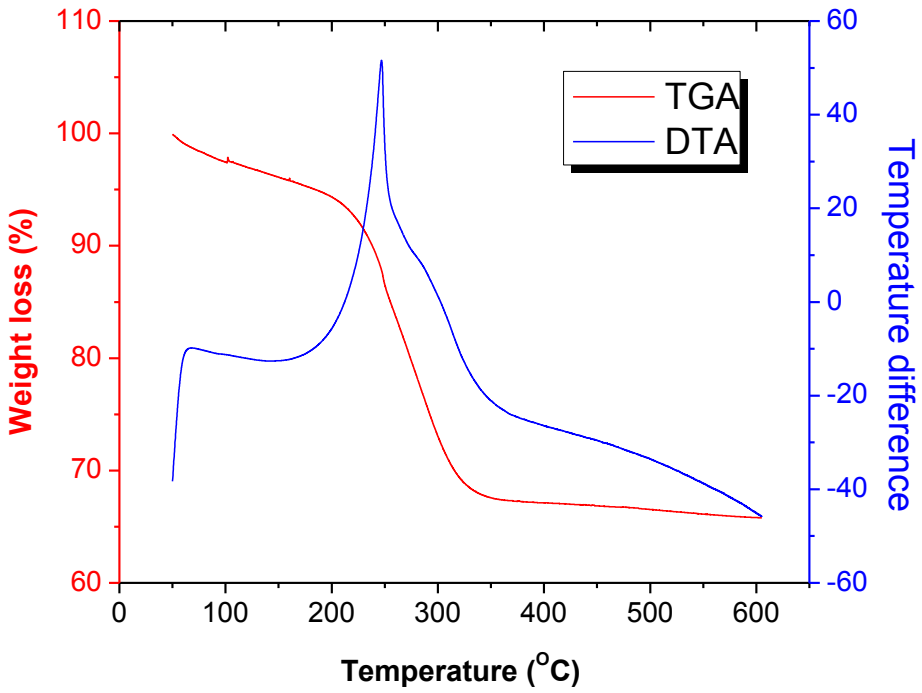

Figure 4.6 TGA/DTA curve of oleic acid coated $MnFe_2O_4$ nanoparticles

4.3 Magnetization Measurements

From figure 4.7, it is clear that as the magnetic field increases, the magnetization of all samples increases and saturates at higher field, which is a typical characteristic of super paramagnetic particles. The saturation magnetization of different sample is given in table 3. It can be observed from table that as the zinc content in the sample increases, the saturation magnetization of the sample decreases. This can be understood from the fact that increasing zinc content will provide greater diamagnetic contribution to the sample. Further for a given sample as the co-precipitation pH increases, the saturation magnetization of the sample also increases. These might be due to increase in particle size as evidenced from table 2.

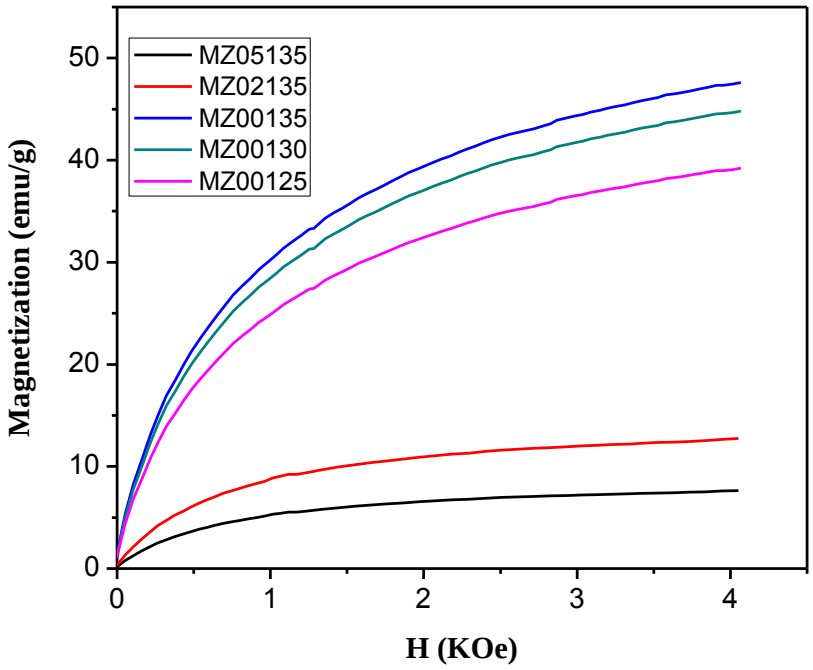

Figure 4.7 Magnetization of $Mn_{(1-x)}Zn_xFe_2O_4$ nanoparticles as a function of magnetic field at different pH

SAMPLE	pH	SATURATION MAGNETIZATION (emu/g)
$MnFe_2O_4$	12.5	39.07
$MnFe_2O_4$	13.0	44.81
$MnFe_2O_4$	13.5	47.42
$Mn_{0.8}Zn_{0.2}Fe_2O_4$	13.5	12.72
$Mn_{0.5}Zn_{0.5}Fe_2O_4$	13.5	7.63

Table 3 Saturation Magnetization of $Mn_{(1-x)}Zn_xFe_2O_4$ nanoparticles at different pH

4.4 Conclusions

- $Mn_{(1-x)}Zn_xFe_2O_4$ nanoparticles are prepared by co-precipitation method at relatively low temperature. Monolayer coating of oleic acid successfully achieved on nanoparticles and they were dispersed in EPK to prepare stable temperature sensitive magneticfluid.
- X-ray diffraction studies indicate that single phase spinel structure nanoparticles are produced with size ranges from 17.5 nm to 20 nm at pH 12.5-13.5.
- TEM analysis indicates that oleic acid coating prevents agglomeration of nanoparticles.
- TGA/DTA analysis reveals 30.4% weight loss that corresponds to monolayer coating of oleic acid.
- VSM analysis reveals that saturation magnetization decreases with the increase in zinc content and saturation magnetization increases with the increase in co-precipitation pH due to increase in particle size.

References

[1] D. Jiles, 'Introduction to magnetism and magnetic materials', Chapman & Hall, London (1991).

[2] D. Craik, 'Magnetism, principles and applications', John Wiley & Sons, Chichester (1995).

[3] E. M. Purcell, 'Electricity and magnetism', McGraw-Hill, New York(1963).

[4] Ping Hu,Hai-bo Yang,De-an Pan,HuaWang,Jian-junTian, Shen-gen Zhang,Xin-feng Wang, Alex A.Volinsky,Journal of magnetism and magnetic materials,322(2010)173–177.

[5] V.G.Bashtovoy, B.M.Berkovsky and A.N.Vislovich, Introduction to magnetic fluids. Washington(1988).

[6] C. Scherer and A. M. FigueiredoNeto, Brazilian Journal of Physics, 35 (2005) 718-719.

[7] K. Raj ,J.Magn.Mater,85(1990)233.

[8] R.V.Mehta,P.PrabhakaranandJ.M.Patel ,J.Instrum Soc. India,15(1985)120.

[9] R.V Mehta and R.VUpadhay,Current science, 76 (1999) 305–311.

[10] A Pankhurst, J Connolly, S K Jones3 and J Dobson, Journal of Physics D Applied Physics, 36 (2003) 170–172.

[11] R.ERosensweig,Ferrohydrodynamics, Dower Publ, Inc, Mineola,N.Z,997.

[12] Hiroshi Yamaguchi, Xin – Rong Zhang, Xiao – Dong Niu, Keisuke Youshikawa, Journal of Magnetism and Magnetic Materials 322 (2010) 698.

[13] B.Jeyadevan, C.N.Chinnasamy, K.Shinoda and K.Tohji, Journal of applied physics, l 93 (2003) 8450-8452.

[14] Hitesh G. Bagaria, Jennifer L. Phillips, David E. Nikles and Duane T. Johnson, Self-Regulated Magnetic Fluids Hyperthermia.

[15] Kuldip Raj, Merrimac; Ronald Moskowitz, Hollis, both of N.H., Magnetic fluids – cooled electromagnetic device and improved cooling method, patent no. 5,462,685, (1995).

[16] Z.G. Zheng, X.C. Zhong, Y.H. Zhang, H.Y.Yu and D.C. Zeng, Journal of Alloys and Compounds, 466 (2008) 377 - 382.

[17] S. M. Attia,Egypt. J. Solids, 29 (2006) 329–340.

[18]Ping Hu, Hai-bo Yang, De-an Pan, Hua Wang, Jian-junTian, Shen-gen Zhang, Xin-feng Wang, Alex A. Volinsky, Journal of Magnetism and Magnetic Materials, 322 (2010) 173–177.

[19]DMakovec,AKo sak1 and M Drofenik, Nanotechnology, 15 (2004) 160 – 166.

[20]Emad M. M. Ewais, Mahmoud M. Hessien and Abdel-Hady A. El-Geassy,J. Aust. Ceram. Soc. 44 (2008) 57-62.

[21] C.Rath, K.K.Sahu, S.Anand , S.K.Date, N.C.Mishra and R.P Das ,Journal of Magnetism and Magnetic Materials , 202 (1999) 77–84.

[22] C. Rath, S. Anand, R.P. Das, K.K. Sahu, S.D. kulkani, S.D. Date, N.C. Mishra, J.Appl.Phys, 91 (2002) 2211.

[23] Jing Feng, Li-Qin Guo, Xiaodong Xu, Shu-Yan Qi, Mi-Lin Zhang, science direct, Physica B, 394 (2007) 100–103.

[24] E.auzans, D.zins, E.blums, R.massart, J.mater.sci.34 (1999)1253.

[25] E.auzans, D. Zins, E Blums, R.massart, Magn. Gidrodin, 36 (1999) 78.

[26] B. Jeyadevan, C.N. Chinnasamy, K. shinoda, K. Tohji, J.Appl. Phys. 93 (2003)8450.

[27] R. Arulmurugana, G. Vaidyanathana, S. Sendhilnathanb and B. JeyadevancPhysica B: Condensed Matter, 368 (2005) 223–230.

[28] B. ParvatheeswaraRao, Chong-Oh Kim, CheolGi Kim, I. Dumitru, L. Spinu, and O.FCaltun , IEEE Transactions on magnetic, 42 (2006) 10.

[29] P. Mathur, A. thakur, M.Singh, J Mater Sci, 42 (2007) 8189 - 8192.

[30] Lai Zhenyu, CSUGangling,ZhenYale, nanoscale Res Let, 2 (2007) 40 -43.

[31] P. Mathur, A.Thakur, M.Singh, J.Mater Sci, 42 (2007) 8189 – 8192.

[32] R.V.Mehta and R.V Upadhyay, Current Science, 76 (1999) 305 – 312.

[33] B Cullity Elements of X-ray diffraction, 2nd Ed Addision - Wesly publication company, USA (1978).

[34] W Wendlandt, Thermal Analysis, John Wiley & Sons Publication (1986).

[35] B Cullity, Introduction to magnetic materials, Addison-Wesley Publication Company, UK (1972).

[36] D Williams, C Carter, Transmission Electron Microscopy: A text book for Materials Science, Springer, USA (2009).

[37] JCPDF card no.74-2402.

[38] Nidhi Andhariya, Bhupendra Chudasama, Rajesh Patel, R V Upadhyay, R V Mehta ,Journal of colloid and Interface Science, 323 (2008) 153 -157.